Journal of Molecular Modeling (2020) 26:172
https://doi.org/10.1007/s00894-020-04427-z

ORIGINAL PAPER

Adenine based molecular junction as biosensor for detection of toxic phosgene gas

Rajan Vohra[1] · Ravinder Singh Sawhney[1] · Jupinder Kaur[1] · Ravinder Kumar[1]

Received: 29 February 2020 / Accepted: 18 May 2020

Abstract

The possibility of adsorption of toxic phosgene gas ($COCl_2$) molecule on one of the nucleobase of DNA—adenine—has been analyzed using the first principle calculations based on density function theory. In accordance with the geometry of the nucleobase, two possible positions have been considered for effective adsorption of gas molecule. The calculations performed on adsorption energies suggest that the gas molecule is able to physisorb at both the considered positions with negligibly small values of charge transfer. The in-depth analysis of electron charge densities depicts that there is no orbital overlapping between the gas molecule and adenine. We observe a significant variation of transport properties of adenine-based molecular junction on adsorption of phosgene molecule while calculation the transport parameters at both the equilibrium as well as non-equilibrium. Also, the variation of HOMO-LUMO gap of adenine molecule on adsorption of phosgene leads to alteration of current and voltage, thus implying that adenine-based sensor can be effectively utilized to sense the presence of phosgene gas in a given environment. Small adsorption energies and recovery time suggest that the rate of desorption of phosgene is very high; thus, the proposed adenine sensor can be effectively used as a highly stable and selective reusable sensor.

Keywords Adenine · DFT · Non-equilibrium Green's function (NEGF) · Sensor · Phosgene gas

Introduction

The enhanced utilization of nano-materials in the last decade for innumerable applications motivated the researchers to extensively explore novel materials along with their uses. The famous lecture by Nobel Laureate Professor Richard P. Feynman "There is plenty of room at the bottom" threw open newer horizons for the researchers to investigate the devices at nanometer-scale utilizing a single molecule [1]. These molecular electronic devices have gained much impetus as they have the tendency to offer a number of advantages in comparison with the silicon-based devices. These molecular devices have the benefits of integration as well as better response times [2]. A highly promising candidate which can be devised in single molecule electronic applications is DNA. The DNA molecule has the property of self-replication which makes it suitable to form similar molecular electronic devices. A single chain of DNA comprises a very long polymer formed by four nucleotides which contain fundamental bases, viz., adenine (A), guanine (G), thymine (T), and cytosine (C). These bases are repetitively attached to the sugar-phosphate backbone. The DNA molecule offers high conductivity and exhibits ohmic behavior when a rope of Lambda-DNA of length 600 nm is considered [3]. A single molecule of poly DNA of length 10 nm sandwiched between metallic leads gives a nonlinear I–V curve [4]. The adenine and guanine nucleobase of DNA connected with gold leads on both the sides, behave as Esaki diodes and show prominent negative resistance behavior [5]. Hanidreza et al proposed zinc and manganese doping in adenine molecule sandwiched between zigzag graphene

Electronic supplementary material The online version of this article (https://doi.org/10.1007/s00894-020-04427-z) contains supplementary material, which is available to authorized users.

✉ Rajan Vohra
rajanvohraece.rsh@gndu.ac.in

Ravinder Singh Sawhney
sawhney_gndu@hotmail.com

Jupinder Kaur
jupinderece.rsh@gndu.ac.in

Ravinder Kumar
ravinder.elec@gndu.ac.in

[1] Department of Electronics Technology, Guru Nanak Dev University, Amritsar, India

electrodes to enhance the spin-splitting phenomenon and conductance [6]. Variations of material and orientations of electrodes have been found to have major impact on the transport properties of DNA [7, 8]. The cytosine nucleobase of DNA is an excellent conductor while guanine nucleobase demonstrate extraordinary negative differential behavior and tunneling phenomenon when sandwiched between metallic leads [9]. DNA-based molecular junctions are an excellent choice to be incorporated as biomarker to sense presence of lead and mercury [10, 11] and to predict abnormalities in the DNA [12]. Though a lot of research has been conducted in the field of molecular junctions based on DNA molecule, yet the application of DNA in sensing of toxic gases has not been fully explored. So in this work, we attempt to explore the usage of one of the strands of DNA, adenine, in sensing a highly toxic phosgene gas. Adenine (A) is one of the purine bases found in nucleic acids. When attached to ribose, it is the nucleoside adenosine (A); when attached to deoxyribose, it is the nucleoside deoxyadenosine (dA) [13]. It is used in forming nucleotides of the nucleic acids. In DNA, adenine binds to thymine via two hydrogen bonds to assist in stabilizing the nucleic acid structures. In RNA, which is used for protein synthesis, adenine binds to uracil. Phosgene (carbonyl dichloride—$COCl_2$) is a colorless gas which is extremely toxic (https://pubchem.ncbi.nlm.nih.gov/compound/Phosgene). Traces of this gas are found naturally due to decomposition of chlorinated compounds. This gas is widely used in the industries for the fabrication of a number of chemicals like pesticides, polycarbonates, isocyanates, dyestuffs, pharmaceuticals, and acid chlorides. Even small dosage of this gas can be fatal for living beings. So it becomes imperative to suggest sensors to detect the leakage of this poisonous gas. These reasons motivate us to explore the usage of DNA nucleobase-based sensor in sensing phosgene gas as given below in subsequent sections. The individual structures of adenine and phosgene and optimized structure of both the molecules have been shown in Fig. 1.

Computational details

In order to perform the necessary calculations, codes incorporated in the non-equilibrium Green's function (NEGF) regime were utilized [14] in combination with density functional theory (DFT) [15–18]. Atomistic Tool Kit along with its graphical interface Virtual Nano Lab is utilized to for modeling and simulating all the configurations [19]. The nucleobase along with the adsorbed phosgene gas molecule was optimized utilizing self-consistent calculations until the forces converged to a value of 0.05 eV/Å at a temperature of 300 K. The molecular junctions are formulated by sandwiching a single adenine molecule and the gas-adenine complexes between gold leads with < 1,1,1 > miller indices to form three different devices. Gold is preferred as the electrode material due to its high stability at room temperature. < 1,1,1 > orientation is chosen for the electrodes as nanowires show stronger conduction behavior alongside this direction [20]. The thus-formed molecular junctions constitute the left and right electrodes with a central scattering region formed between them. The central scattering region encompasses an extended molecule with some part of the electrodes included alongside the molecule to augment stronger coupling [21]. Double-zeta polarized basis set [22] is utilized for the nucleobase-gas complex while single-zeta polarization is utilized for gold atoms as it is found to give better results in previously published works [23]. The calculations were performed utilizing generalized gradient approximation (GGA) correlation functional of Perdew-Burke-Ernzerhof as these are dependent on the localized value of electron density and gradient [24]. In order to calculate the transport properties in the low voltage regime, we have utilized Landauer-Imry system of elastic scattering in conjunction with the NEGF. To calculate the current, electron density matrix is formulated by first solving the NEGF in self-consistent manner followed by calculation of electrostatic potential [25].

The I–V curve can be calculated by exploiting Landauer-Buttiker formalism which employs the transmission probability $\{T(E,V)\}$ to predict the relationship between the applied voltage and current as given below [25]:

$$I(V) = 2\frac{e}{h}\int_{\mu_L}^{\mu_R} T(E,V)[f(E-\mu_L)-f(E-\mu_R)]dE \quad (1)$$

In the above equation, μ_L/μ_R signifies the electrochemical potential of left/right electrode and $T(E,V)$ denotes the transmission function. To determine the transmission function, adequate knowledge about the amount of coupling amongst the molecule and the electrodes along with the information about the location of the molecular energy levels is sufficient criterion. In the study at hand, the transmission was determined in a similar manner as [26]:

$$T^k(E,V) = T_r\left[\Gamma_1^k(E,V)G_M^k(E,V)\Gamma_2^k(E,V)G_M^{k'}(E,V)\right] \quad (2)$$

Here, Γ (E) denotes the coupling function. It proficiently delivers knowledge about the type of contact between the considered molecule and the metallic leads and G_M (E,V) represents the Green's function. It can be presumed that the molecular energy levels have the propensity to float aloft with a value eV_{mol} which is roughly comparable with the value of electrostatic potential of the considered molecule. For ease, it can be approximated that the molecular energy levels are stable while the substrate on the other hand has a capability to float downwards by eV_{mol}. Consequently, the values of electrostatic potentials of both the electrodes can be calculated as given below [27]:

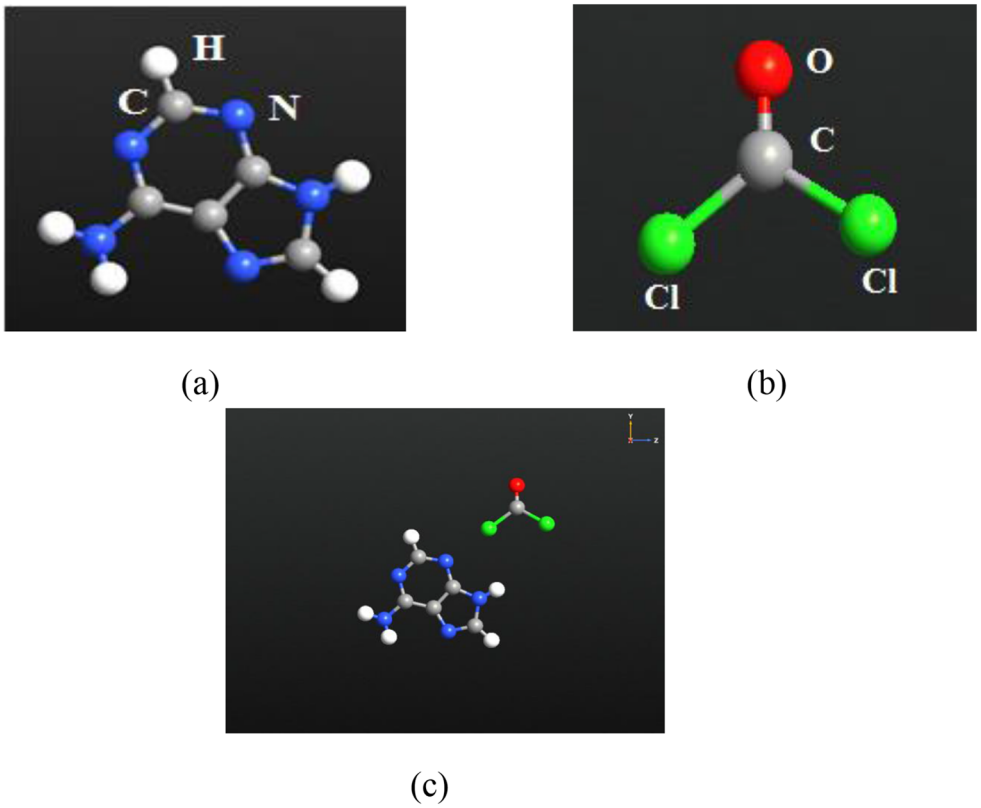

Fig. 1 Molecular representation of **a** adenine (C5H5N5), **b** phosgene ($COCl_2$), and **c** optimized structure of both the molecules

$$\mu_L = E_F - eV_{mol} = E_F - \eta eV \quad (3)$$

$$\mu_R = E_F - eV + eV_{mol} = E_F + (1-\eta)eV \quad (4)$$

In the equations given above, E_F represents the equilibrium Fermi energy, e denotes the charge on an electron, and η is useful in providing information as to how the potential difference (V) is distributed amongst the two metallic electrodes. It can be calculated as: $\eta = V_{mol}/V$. From previously implemented methods utilizing a scanning tunneling microscope, it has been inferred that η can be adjusted to around 0.5 by suitably fine-tuning the contacts in a proportioned position [26–28]. η is a valuable parameter to describe the potential profile of molecules in molecular junctions.

Next, the differential conductance can be contemplated as follows:

$$G = \frac{I(V_R, T_L, T_R) - I(V_L, T_L, T_R)}{V_R - V_L} \quad (5)$$

Results and discussion

To contemplate the electronic properties of nucleobase of DNA with adsorbed gas molecule, total energies, adsorption energies, charge transference, and electron density are determined. Furthermore, the quantum transport phenomenon is explored by comprehending the density of states (DOS), chemical potential, transmission spectra, HOMO-LUMO gap, molecular energy spectra, Eigen states, I–V curve, and differential conductance.

Total energies and adsorption energies

From the base pair A–T of DNA, adenine gives best quantum transport behavior [12]. Adenine molecule comprises rings formulated by nitrogen, carbon, and hydrogen atoms ($C_5H_5N_5$). As the gas molecule can adsorb at any position on the nucleobase, we have taken two most favorable positions present vertically, since the phosgene molecule interacts readily with the nitrogen atom of adenine at these two locations, namely position A and position B. The structures formed post adsorptions of gas molecule on the nucleobase are completely relaxed. The complete transitions states and score plot for the phosgene adsorption at both the favorable sites of adenine are shown in Fig. 2. The score plot gives information about the most significant transition states in the trajectory when phosgene is adsorbed on the surface of adenine at positions A and B, respectively. The phosgene molecule takes greater time and undergoes more number of transitions when it is adsorbed at position B in comparison with adsorption at position A.

This is followed by determination of adsorption energies which is an important parameter to garner

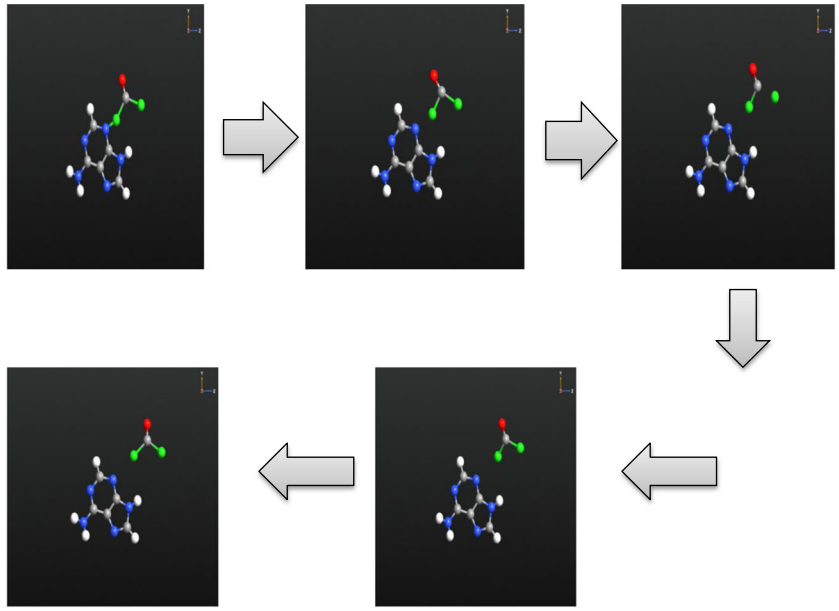

(a)

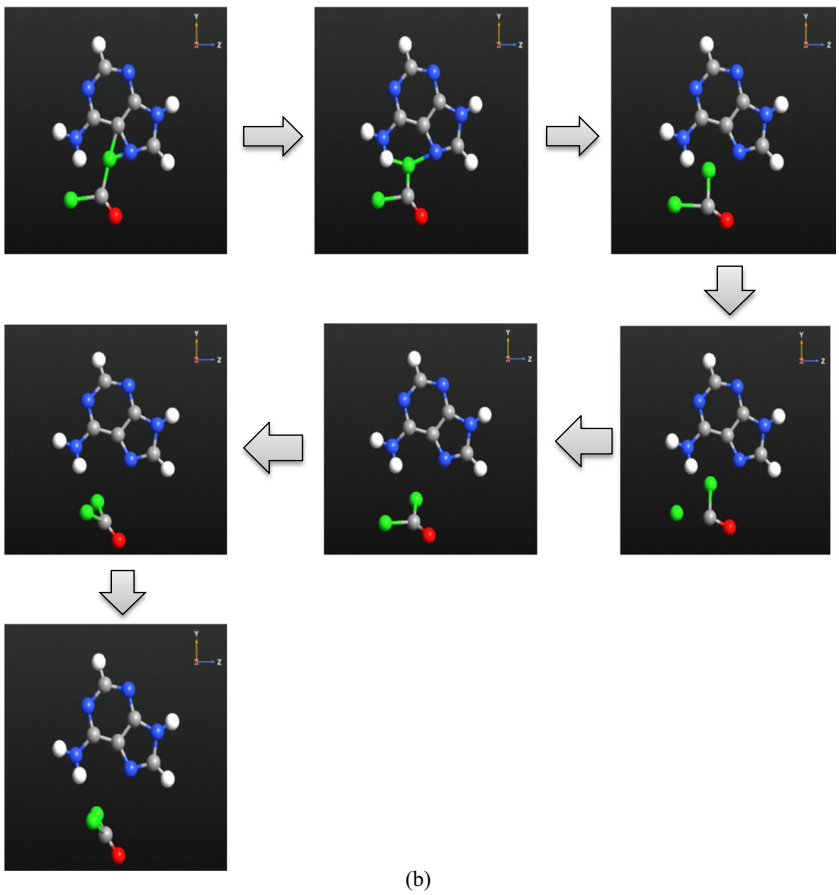

(b)

Fig. 2 Transition states for adsorption of phosgene molecule on adenine at **a** position A, **b** position B, and **c** score plot

knowledge about the kind of interaction between the phosgene molecule and adenine. Positive value of adsorption energy represents repulsion while negative value denotes attraction. The more the negative value of adsorption energy, the better is the adsorption. The optimized structures of phosgene-adenine with the least energies are as given in Fig. 3. The adsorption energy is determined using the following formula:

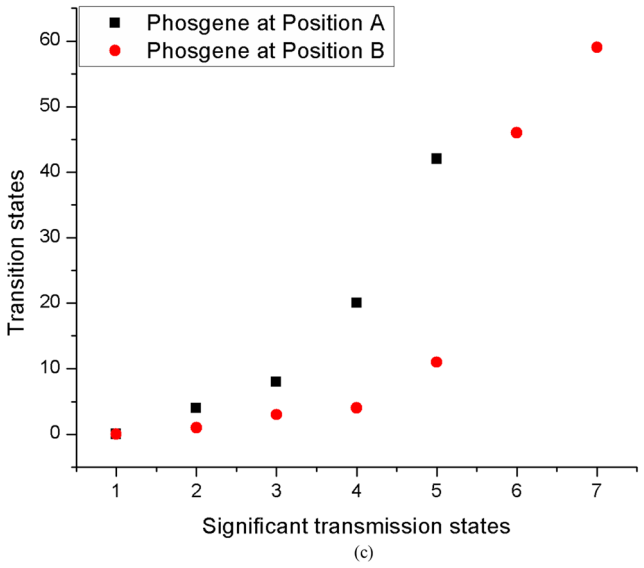

(c)

Fig. 2 continued.

$$E_{ad} = E_{(adenine+phosgene)} - E_{adenine} - E_{phosgene} \quad (6)$$

In the above equation, E_{ad} denotes the adsorption energy, $E_{(adenine + phosgene)}$ represents total energy of adenine-phosgene complex, and $E_{adenine}$ and $E_{phosgene}$ are the total energies of adenine and phosgene molecules, respectively. The values of total energies and adsorption energies of both the adenine-phosgene complexes are tabulated in Table 1.

Adsorption of phosgene at position A

When the phosgene molecule is adsorbed at position A of the nucleobase, there is a slight decline in bond angle from 34.52 to 34.42°. The O–C and C–Cl bond length remains almost at same value of 1.19 Å and 1.75 Å, respectively. Thus, the phosgene molecule is adsorbed on the adenine molecule in a non-dissociative way and no visible chemical bond formation occurs between the gas and nucleobase. The binding distance which is defined as the smallest distance between the adsorbent and gas molecule is found to be 2.78 Å. The adsorption energy is calculated as − 0.36 eV and a charge transfer of 0.023e occurs between the gas and nucleobase. Thus, very less value of adsorption energy and charge transfer denotes that the phosgene molecule is physisorbed on the adenine molecule.

Table 1 Total energies and adsorption energies of gas and nucleobase complexes

Structure	Total energy (eV)	Adsorption energy (eV)
Adenine	− 2223.43560	-
Phosgene	− 1507.42291	-
Phosgene at position A	− 3731.22192	− 0.36
Phosgene at position B	− 3731.31331	− 0.45

Adsorption of phosgene at position B

When the gas molecule is adsorbed at position B of the DNA strand, the bond angles lowers to a value of 34.01° and the O–C and C–Cl bond length remains almost constant at 1.19 Å and 1.75 Å, respectively. The binding distance is found to be 2.70 Å. The adsorption energy is determined as − 0.45 eV with a charge transfer of 0.041e. Thus, the gas molecule is physisorbed at position B of the nucleobase in a non-dissociative manner.

Thus, from the analysis of adsorption energies, we deduce that the phosgene molecule is physisorbed at both positions A and B of the DNA strand. The observed adsorption is very important to decide whether the sensor can be deployed for single or multi-use. For physisorption, the sensor can be deployed multi-time, but on the other hand, if the adsorption is chemisorb, it can only be utilized for single time. As physisorption is noticed in our phosgene-adenine structure, thus, it can be deployed as a reusable sensor.

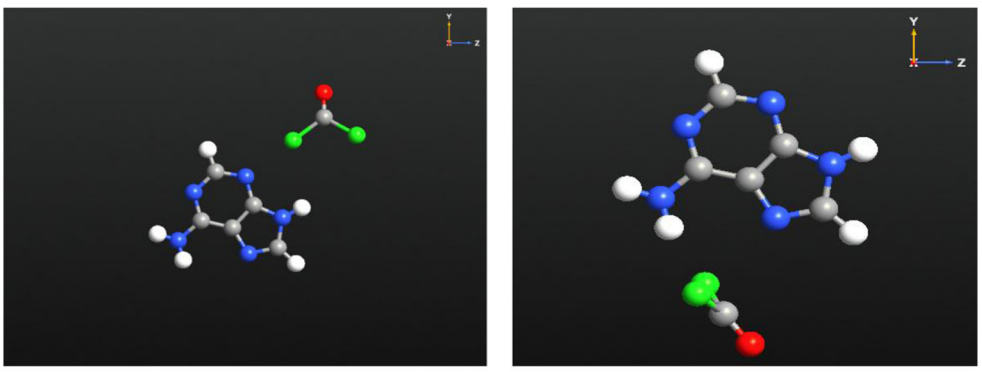
(a) (b)

Fig. 3 Optimized structure of phosgene adsorbed on the surface of adenine at **a** position A and **b** position B

Electron charge density

To further scrutinize the adsorption phenomenon of phosgene gas on the nucleobase, we contemplate the electron charge densities of the gas-nucleobase devices as portrayed in Fig. 4. From the figure, it is clearly visualized that in both the cases, no overlapping between the orbitals of the adsorbate and adsorbent is visible. No overlapping along with the little charge transfer further supports the fact that phosgene is physisorbed on the surface of adenine. Thus, this phenomenon plays a very significant role in defining the sensing capacity of adenine.

Transport properties

Next, the quantum transport properties of gas-nucleobase devices are determined under both the equilibrium and non-equilibrium conditions and finally compared with pristine adenine device. Figure 5 shows the molecular junction for all the cases.

Quantum transport at equilibrium

Firstly, to gather information about the transport properties, density of states (DOS) is determined for all the molecular junctions. DOS provides significant details about the states actively contributing in transmission. Figure 6 assays the comparative density of states of pure adenine and gas-adenine devices.

When phosgene is adsorbed at position A, a very sharp peak is visible around 0.3 eV. Sharp peak signifies lesser transmission. Also, LUMO is closer to fermi level (0 eV), thus dominating the transmission. For phosgene adsorption at position B, the curve is identical in shape to that of pure adenine. Broader peaks are visualized confirming better transmission in both the cases in comparison with phosgene adsorption at position A. For both the devices, LUMO orbital is in close proximity with the fermi level, thus assuring the dominant behavior of LUMO orbital in transmission. In regard to the Lorentzian formalism, the probability of transmission is dependent on two factors, viz. the amount of orbital broadening due to the coupling between the central molecule with the metallic leads and the orbital alignment in respect to the fermi level. These factors are dependent on fermi level which is further reliant on the chemical potential. Thus, a direct relationship between the chemical potential and transmission probability can be given as follows [29, 30]:

$$T(E) = \frac{\left(\frac{\tau}{2}\right)^2}{\left[(E-E_F)^2 + \left(\frac{\tau}{2}\right)^2\right]} \tag{7}$$

Beebe et al. comprehended the relationship between the barrier potential and transmission [31, 32]. Thus, the chemical potential is determined to get insight into the quantum transport. The values of chemical potential are −2.30 eV, −2.30 eV, and −4.51 eV for pure adenine, adenine with gas at position A, and adenine with gas at position B, respectively. The chemical potential is an important factor to determine the relation between work function and the probability of transmission. Thus, it can be inferred that lesser value of work function is assayed by adenine with gas at position B while almost same value of work function is portrayed by pure adenine and adenine with gas at position A. Higher the value of work function implies greater energy requirement for adding or removing electron from the system [32]. Thus, we infer that transmission probability will be more in the device with gas positioned at B as it has least value of work function.

Next, the transmission spectra are analyzed for all the molecular junctions. The positioning of the molecular orbitals along with the type of interaction between the central molecule and metallic leads can be determined by exploring the DOS and transmission spectra curves at equilibrium. The transmission spectra at zero bias for all

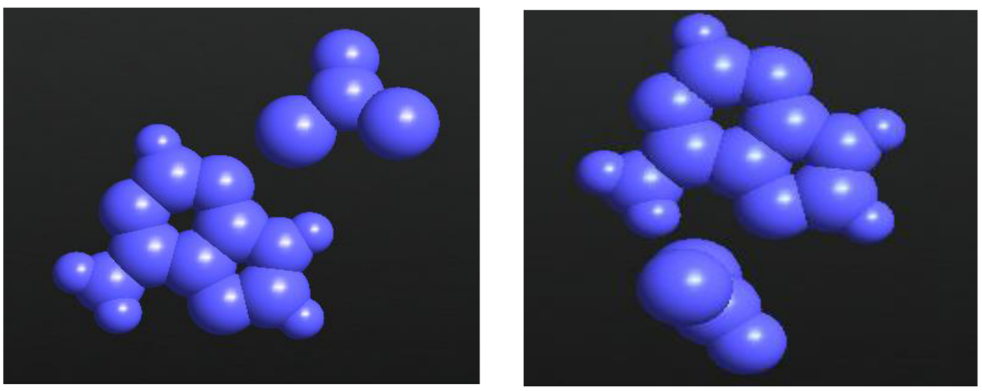

(a) (b)

Fig. 4 Electron density of phosgene-adenine complex with phosgene at **a** position A and **b** position B

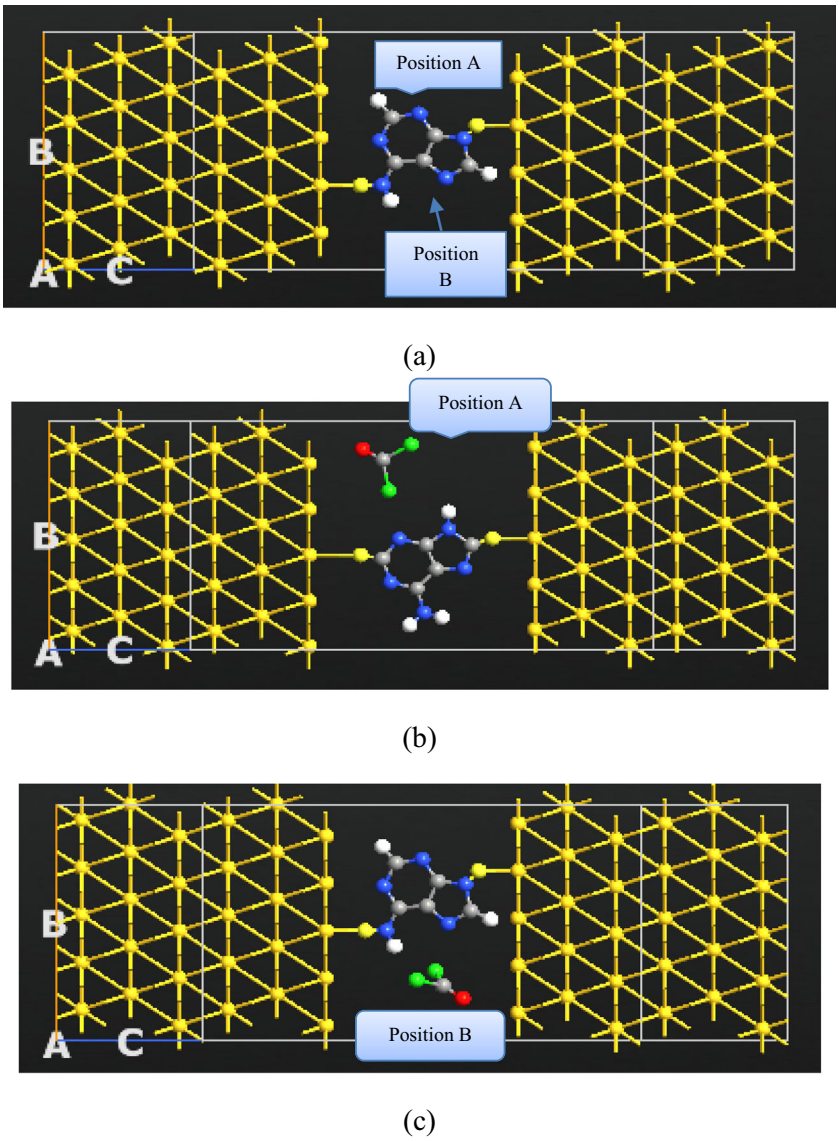

Fig. 5 Molecular junction formed using gold electrodes for **a** pure adenine **b** Phosgene-Adenine complex with phosgene adsorbed at position A. **c** Phosgene-Adenine complex with phosgene adsorbed at position B

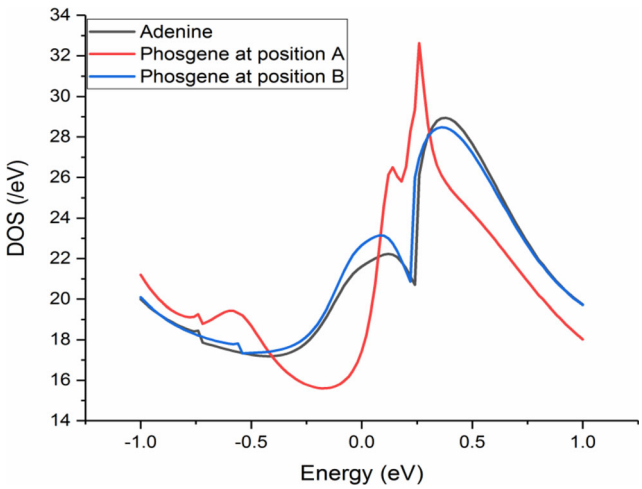

Fig. 6 Density of states (DOS) for all the devices under consideration

the junctions are as shown in Fig. 7. The transmission spectra are utilized to garner information about the HOMO-LUMO gap and the orbitals playing significant role in transmission. From the analysis of graphs given in the figure, we observed that for all the junctions, LUMO orbitals are sharper and closer to fermi level and thus play a dominant role in transmission. Transmission spectra also gave us insight about the molecular orbital playing significant role in transmission. Broader transmission peaks are visualized in case of pure adenine and gas-adenine device oriented at position B. Broader peaks refer more coupling between the central molecule and the metallic leads, thus enhancing the transmission. In contrast to this, very sharp peaks are visualized in the transmission spectra of gas-adenine device positioned at A, thus implying poorer coupling resulting in lesser transmission.

Table 2 HOMO, LUMO, and HLG (Homo-Lumo gap) in all the molecular junctions

Molecule	HOMO (eV)	LUMO (eV)	HOMO-LUMO gap (eV)
Adenine	− 1.23	0.54	1.77
Phosgene at position A	− 0.22	1.95	2.17
Phosgene at position B	− 1.12	0.57	1.69

Further, the molecular energy spectra of gas-adenine devices are determined at equilibrium. The HOMO, LUMO, and HOMO-LUMO gap are tabulated in Table 2.

The values in the above table deduced that HLG (Homo-Lumo gap) is the highest in case of phosgene-adenine device (position A) while the least value of HLG is portrayed by device formed by phosgene-adenine device (position B). Pure adenine device assay HLG has the value in between. Thus, from the analysis of HLG, we revealed that the transport properties of adenine have been altered on adsorption of phosgene molecule at both the considered positions.

Furthermore, the pictorial representation of Eigen states of HOMO and LUMO is shown in Fig. 8. In case of pure adenine, the delocalization of HOMO orbitals are at the anchor positions, while for LUMO orbital, it is more pronounced on the right side of the anchor position. Sigma bonds are dominating in case of HOMO in comparison with the pie bonds visualized in LUMO orbitals. For phosgene-adenine device (position A), the delocalization is shown on the right side of scattering region for HOMO orbitals, while the LUMO orbital gives eminent delocalization on the left side. In addition to this, LUMO orbitals have higher

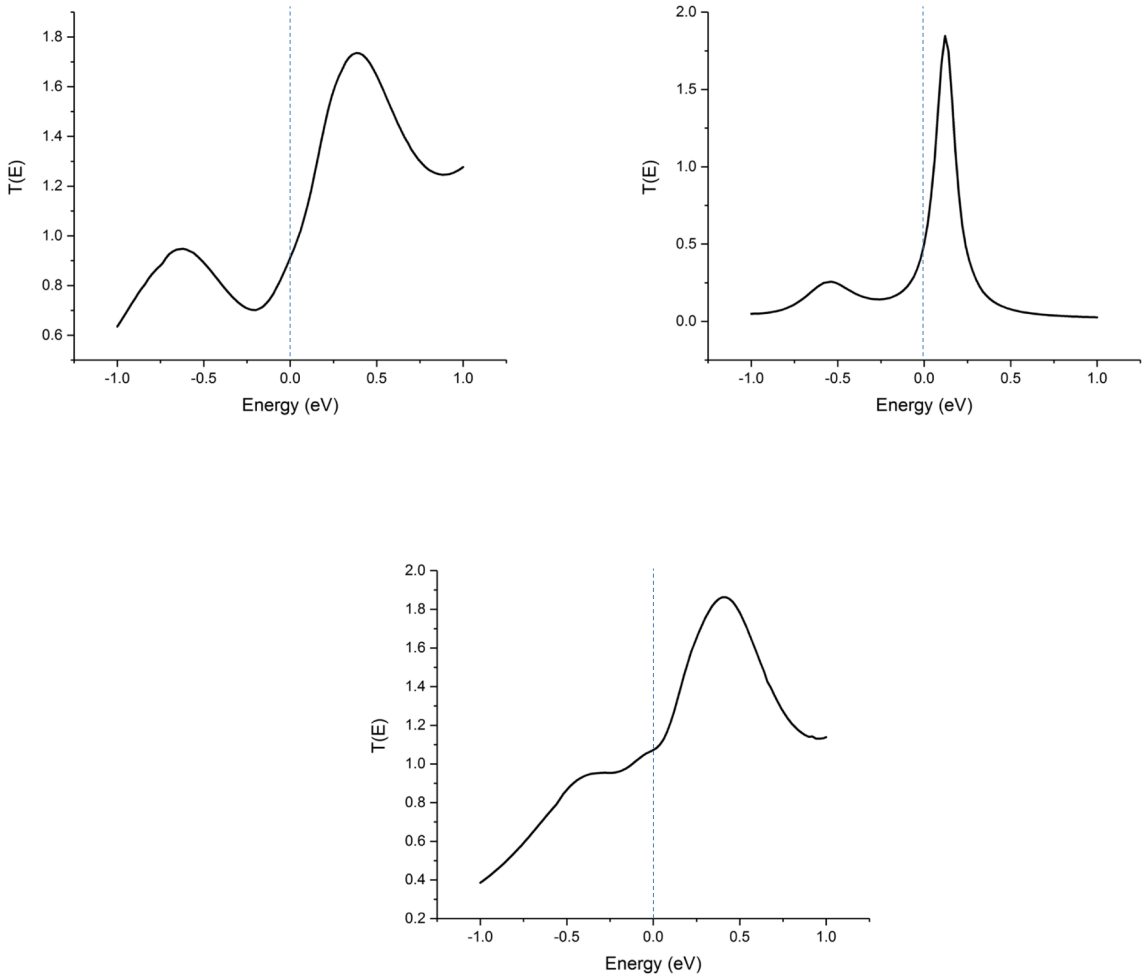

Fig. 7 Transmission spectra at 0 V for molecular junction comprising **a** pure adenine, **b** Adenine-Phosgene complex with phosgene adsorbed at position A, **c** Adenine-Phosgene complex with phosgene adsorbed at position B. The dotted line in all the figures represents the fermi level (0 V)

delocalization behavior. For phosgene-adenine device (position B), the similar kind of behavior for HOMO-LUMO orbital delocalization has been observed with both sigma and pie bonds participating in transmission. Thus, the results obtained from the Eigen states are in complete agreement with the DOS and transmission spectra as shown in Figs. 6 and 7.

Quantum transport under non-equilibrium conditions

To further analyze the quantum transport behavior, the I–V curve and differential conductance are comprehended at different voltages ranging from − 1 to 1 V considering a step size of 0.5 V. In this context, the I–V curve is plotted as shown in the Fig. 9a. From the current-voltage curve, we have observed that the highest value of the current is noticed in phosgene-adenine device (position B), while for phosgene-adenine device (position A), least amount of current is assayed. Intermediary current is portrayed by pure adenine device. This is because the HOMO-LUMO gap is highest in case of gas-nucleobase device positioned at A while least value is depicted by gas-nucleobase device positioned at B. The higher the value of HLG, the lower is the current and vice versa. Thus, our results are in complete agreement with the HLG shown in Table 2. In addition to this, the strong coupling bond has been observed between molecule and electrodes in case of phosgene-adenine device (position B) and pure adenine; thus, both these devices assay higher current. Our results are also in agreement with the values of work function

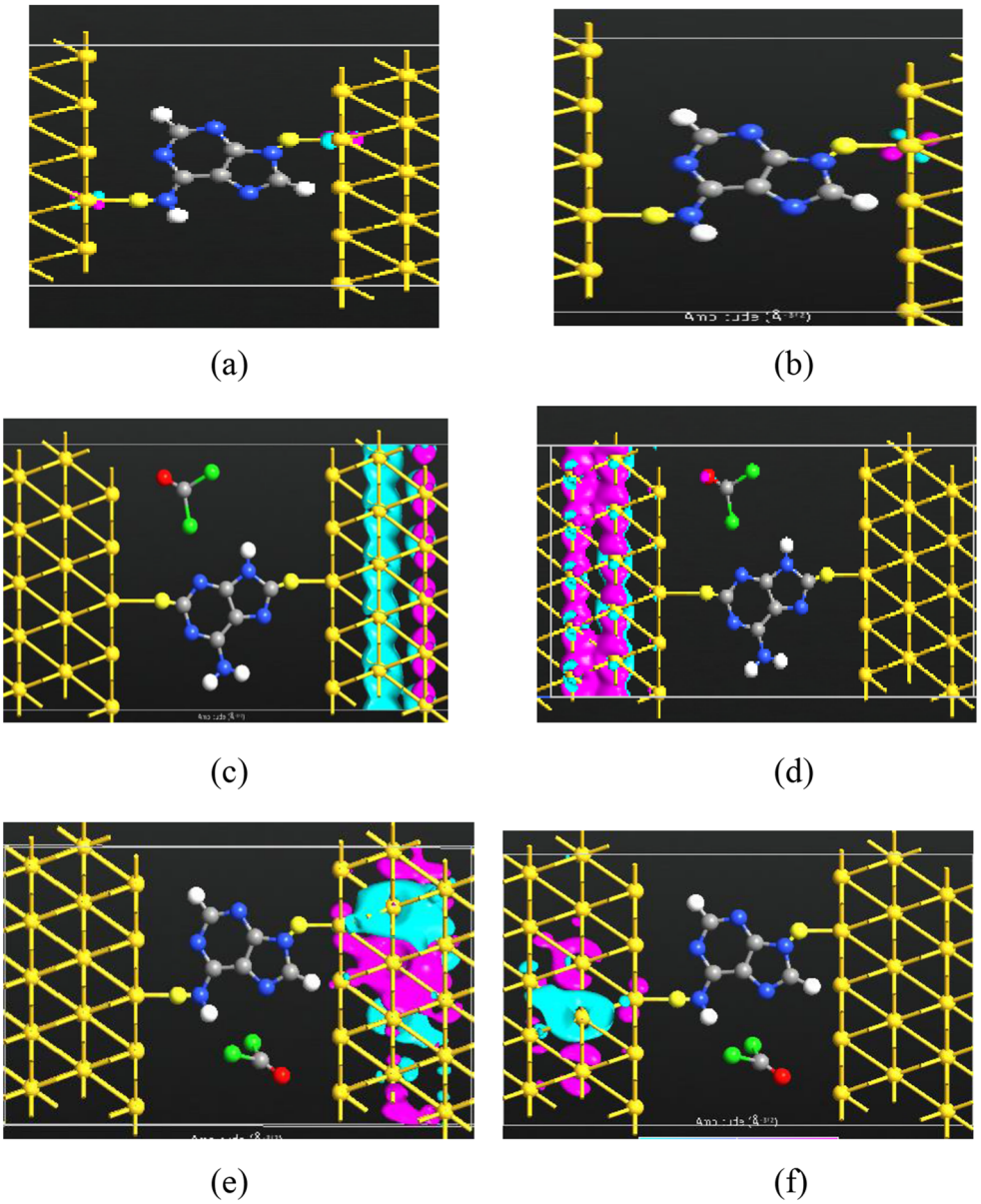

Fig. 8 Eigen states of **a**, **b** HOMO and LUMO of pure adenine device; **c**, **d** HOMO and LUMO of phosgene-adenine device (position A); and **e**, **f** HOMO and LUMO of phosgene-adenine device (position B)

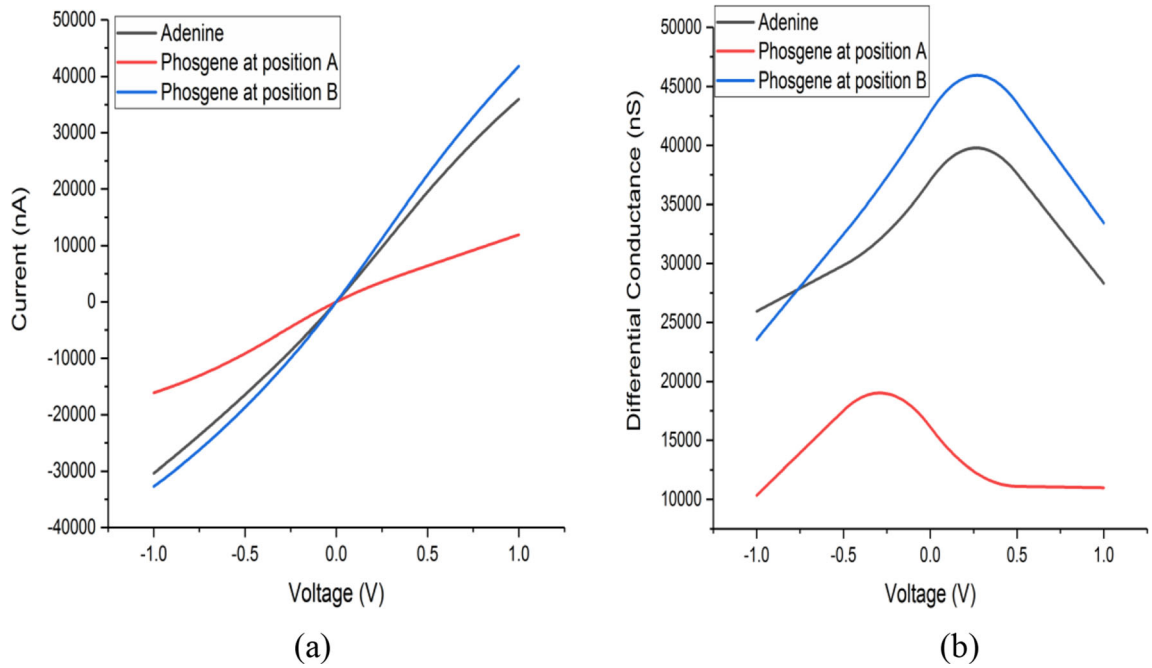

Fig. 9 **a** I–V curve. **b** Differential conductance for all the molecular junctions

calculated earlier. Although the work function is the same in case of pure adenine and phosgene-adenine device (position A), yet pure adenine device gives larger current as coupling in this device is stronger in comparison with the latter. From the analysis of I–V curve, we also deduce that current varies after adsorption of phosgene gas on adenine; thus, adenine can be deployed for possible sensing application of phosgene gas.

This is followed by calculation of differential conductance. The differential conductance for all the junctions is as shown in Fig. 9b. From the graph, we deduce that highest differential conductance is assayed by phosgene-adenine complex with gas adsorbed at position B, followed by pure adenine and least conductance is observed by phosgene adsorbed at position A of the nucleobase. It can also be clearly seen that in case of pure adenine and phosgene adsorption at position B, the differential conductance curve is completely identical. Thus, the results obtained here are also in agreement with those of the I–V curve.

Feasibility of adenine for possible application in sensing toxic phosgene gas

To design a practical sensor, it is necessary to overcome a few challenges like stability, selectivity, sensitivity, and speed (which is defined in terms of recovery and response rates) [33]. The adenine nucleobase is highly stable at room temperature. It has been noticed that even on adsorption of the phosgene gas molecule at both the considered positions, the adenine molecule retains its structure and no deformation is visible. This specifies the stability of adenine even on adsorption of toxic phosgene gas. In order to get insight about the sensitivity and selectivity of adenine molecule in sensing toxic phosgene gas, we have explored the adsorption phenomenon of gas molecule at two positions as stated above. As we have seen in Figs. 3, 4, and 9a, adenine can sense phosgene molecule at both positions A and B, thus implying that adenine can be used as a highly sensitive and selective sensor for detecting phosgene gas at its entire surface.

Furthermore, in order to scrutinize the dependence of recovery time on the adsorption energy, we have utilized transition state theory as follows:

$$\tau = \nu_0^{-1} e^{-E_{\mathrm{ads}}/KT} \tag{8}$$

In the above equation, T denotes temperature, K represents Boltzmann's constant (8.62×10^{-5} eV/K), and ν_0 is attempt frequency. Peng et al. used this method to determine the recovery time for sensing NO_2 utilizing carbon nanotubes (CNTs) [34]. It was inferred that for adsorption energies in the range − 0.34 to − 0.79 eV, the recovery time varies from 5 μs to 16 s at room temperature. In addition, the recovery time was found to be 12 h for adsorption energy of − 1.00 eV. Assuming that the value of attempt frequency is same for NO_2 and phosgene gas ($\nu_0 = 10^{12}$ s^{-1}), we determine the recovery time for phosgene gas at room temperature (300 K) [33]. For phosgene adsorption at position A of the nucleobase, the recovery time is 1.11 μs, while for adsorption at position B, the recovery time is 36 μs. Very small value of adsorption energy and recovery time confirms ease of desorption of phosgene molecule. Thus, adenine can be used as a reusable sensor for sensing phosgene gas as the desorption phenomenon is fast.

Thus, by analyzing total energies, adsorption energies, charge transference, electron density, density of states (DOS), chemical potential, transmission spectra, HOMO-LUMO gap, molecular energy spectra, Eigen states, I–V curve, and differential conductance, we conclude that adenine can be effectively employed as a reusable sensor for sensing toxic phosgene gas.

Conclusion

The density functional theory in combination with the non-equilibrium Green's function approach has been utilized to explore the likelihood of utilizing adenine nucleobase to detect the presence of toxic phosgene gas in the environment. Calculation of adsorption energy and charge transfer after adsorption of phosgene at two different positions on the adenine molecule suggests physisorption of the gas on the surface of the nucleobase. The electron density analysis visualizes the non-overlapping orbitals of the gas and the nucleobase, thus further implying the occurrence of physisorption. The DOS and transmission spectra analysis at equilibrium reveals that LUMO orbital plays a dominant role in transmission in all the considered junctions. The HLG varies significantly after the adsorption of phosgene gas resulting in noticeable variation in the I–V curve and conductance. Therefore, adenine molecular junction can be suitably employed in sensing phosgene gas. In addition, very small values of adsorption energies and recovery time result in faster desorption. Thus, adenine is a promising material to be utilized in formulating a highly stable and selective reusable sensor for detecting phosgene gas.

Acknowledgments We gratefully acknowledge the "Ministry of Electronics and Information Technology," Government of India, for initiating Visvesvaraya PhD Scheme. The authors would also like to thank Synopsys for their valuable support.

Compliance with ethical standards

Conflict of interest The authors declare that they have no conflict of interest.

References

1. Feynman RP (1992) There is plenty of room at the bottom. J Mems 1:60
2. Tour J, Kozaki M, Seminario JM (1998) Molecular scale electronics: a synthetic/computational approach to digital computing
3. Fink HW, Schonenberger C (1999). Nature (London) 398:407
4. Porath D, Bezryadin A, de Veries S, Dekker C (2000). Nature (London) 403:635
5. Randhawa DKK, Bharadwaj LM, Singh ML (2011). Int J Comput Appl 17:8
6. Simchi H, Esmaeilzadeh M, Hossein Mazidabadi J (2014). Appl Phys 115:044701
7. Vohra R, Bhat Y, Kaur M, Sawhney RS (2017) Scrutiny of electron transport properties of adenine molecule under dissimilar miller orientations. J Bionanosci 11(5):363–369
8. Bhat Y, Vohra R, Kaur M, Sawhney RS (2017) Impact of different metallic electrodes on quantum transport through deoxyribonucleic acid. J Comput Theor Nanosci 14(8):4137–4142
9. Vohra R, Sawhney RS (2018) Comparative evaluation of NANO transport properties for DNA nucleobase based molecular junction devices. J Mol Model 24(11):330
10. Vohra R, Sawhney RS (2018) Adenine based molecular biomarker for the diagnosis of Lead and mercury presence in a live sample. J Nanoelectron Optoelectron 13(4):554–561
11. Kaisti M (2017) Detection principles of biological and chemical FET sensors. Biosens Bioelectron 98:437–448
12. Vohra R, Sawhney RS (2018) Envisaging quantum transport phenomenon in a muddled base pair of DNA. Pramana 90(5):58
13. Definition of adenine from the genetics home reference-National Institutes of Health
14. Taylor J, Brandbyge M, Stokbro K (2002) Theory of rectification in tour wires: the role of electrode coupling. Phys Rev Lett 89(13): 138301
15. Lang ND (1995) Resistance of atomic wires. Phys Rev B Condens Matter Mater Phys 52(5335)
16. Xue Y, Datta S, Ratner MA (2002) First-principles based matrix Green's function approach to molecular electronic devices: general formalism. Chem Phys 281(151)
17. Brandbyge M, Mozos JL, Ordejon P, Taylor J, Stokbro K (2002) Density-functional method for non-equilibrium electron transport. Phys Rev B Condens Matter Mater Phys 65(165401)
18. Taylor J, Guo H, Wang J (2001) Ab initio modeling of quantum transport properties of molecular electronic devices. Phys Rev B Condens Matter Mater Phys 63(245407)
19. Atomistic Toolkit Manual, Quantumwise Inc. Atomistix toolkit version 13.8.0, Quantumwise A/S (http://quantumwise.com)
20. Reed MA, Zhou C, Muller CJ, Burgin TP, Tour JM (1997) Conductance of a molecular junction. Science 278:252–254. https://doi.org/10.1126/science.278.5336.252
21. Walia GK, Randhawa DK (2018). Struct Chem 29:257. https://doi.org/10.1007/s11224-017-1025-9
22. Kaur J, Kumar R, Vohra R, Sawhney RS (2020) A pursuit to design highly sensitive fullerene-based sensors: adsorption and dissociation phenomenon of toxic sulfur gases on B_{40} fullerene. J Mol Model 26:17
23. Vohra R, Sawhney RS (2018) Contemplating nanometer scale transport characteristics through aromatic molecules based molecular devices. Int J Nanoelectron Mater 11(3):333
24. Perdew JP, Burke K, Ernzerhof M (1996) Generalized gradient approximation made simple. Phys Rev Lett 77:3865. https://doi.org/10.1103/PhysRevLett.77.3865
25. Landauer R (1989) Conductance determined by transmission: probes and quantized constriction resistance. J Phys Condens Matter 1:8099
26. Heurich J, Cuevas JC, Wenzel W, Schon G (2002) Electrical transport through single-molecule junctions: from molecular orbitals to conduction channels. Phys Rev Lett 88:256803. https://doi.org/10.1103/PhysRevLett.88.256803
27. Lawson JW, Bauschlieher CW (2006) Transport in molecular junctions with different metallic contacts. Phys Rev B Condens Matter Mater Phys 74:125401. https://doi.org/10.1103/PhysRevB.74.125401
28. Datta S (1995) Electronic transport in mesoscopic systems. Cambridge University Press, Cambridge

29. Kuwabara T, Sugiyama, Yamaguchi, Takahashi (2009) Inverted type bulk-heterojunction organic solar cell using electro-deposited titanium oxide thin films as electron collector electrode. Thin Solid Films 517:3766. https://doi.org/10.1016/j.tsf.2008.12.039
30. Paulsson M, Datta S (2003) Thermoelectric effect in molecular electronics. Phys Rev B Condens Matter Mater Phys 67(24): 241403. https://doi.org/10.1103/PhysRevB.67.241403
31. Beebe JM, Kim B, Gadzuk JW, Frisbie CD, Kushmerick JG (2006) Transition from direct tunneling to field emission in metal-molecule-metal junctions. Phys Rev Lett 97:026801. https://doi.org/10.1103/PhysRevLett.97.026801
32. Beebe JM, Kim B, Gadzuk JW, Frisbie CD, Kushmerick JG (2008) Measuring relative barrier heights in molecular electronic junctions with transition voltage spectroscopy. ACS Nano 2:827. https://doi.org/10.1021/nn700424u
33. Yong Y, Cui H, Zhou Q, Su X, Kuang Y, Li X (2017) Adsorption of gas molecules on graphitic GaN sheet and its implications for molecule sensors. RSC Adv 7:51027. https://doi.org/10.1039/c7ra11106a
34. Peng S, Cho K, Qi P, Dai H (2004) Ab initio study of CNT NO_2 gas sensor. Chem Phys Lett 387:271–276. https://doi.org/10.1016/j.cplett.2004.02.026